ACS Photonics

Article

pubs.acs.org/journal/apchd5

Symmetry Breaking in Tetrahedral Chiral Plasmonic Nanoparticle Assemblies

Vivian E. Ferry,[†] Jessica M. Smith,[‡] and A. Paul Alivisatos*[,†,‡]

[†]Materials Science Division, Lawrence Berkeley National Laboratory, 1 Cyclotron Road, Berkeley, California 94720, United States

[‡]Department of Chemistry, University of California—Berkeley, Berkeley, California 94720, United States

Supporting Information

ABSTRACT: Self-assembled plasmonic structures combine the specificity and tunability of chemical synthesis with collective plasmonic properties. Here we systematically explore the effects of symmetry breaking on the chiroptical response of an assembly of plasmonic nanoparticles using simulation. The design is based on a tetrahedral nanoparticle frame with two different types of nanoparticles, where chirality is induced by targeted stimuli that change the distance along one edge of the assembly. We show that the intensity, spectral position, and handedness of the CD response are tunable with small structural changes, making it usable as a nanoscale plasmonic ruler. We then build upon this initial design to show that the symmetry breaking principle may also be used to design a chiral pyramid using a mixture of different nanoparticle materials, which affords tunability over a broad spectral range, and retrieves nanoscale conformational changes over a range of length scales.

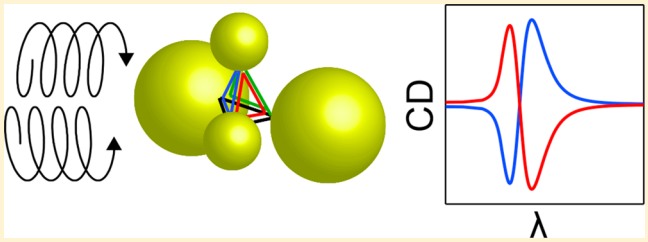

KEYWORDS: *plasmonics, circular dichroism, optical chirality, numerical simulation, self-assembly*

Chiral molecules are essential to biological systems and have found widespread application in pharmaceuticals, asymmetric synthesis, and catalysis.[1] Characteristically, chiral molecules exhibit circular dichroism (CD), the differential absorption of left and right handed circularly polarized light. Analogously to molecular systems, inorganic chiral plasmonic structures can be designed by controlling the spatial placement of achiral nanoparticles in an assembly, as recently demonstrated in structures such as helices, pyramids, and twisted nanorod pairs.[2−10] Notably, the figure of merit for chirality, defined as the ratio of the CD signal to the extinction, can be considerably larger in plasmonic systems than in molecular systems. Chiral nanostructures have been proposed for applications including negative index media, broadband circular polarizers, slow light applications, and enantioselective photochemistry.[11−13]

Chiral assemblies of plasmonic nanoparticles are part of a larger class of self-assembled metamaterials, where optical signatures may be actively tuned and switched through interations with external stimuli.[14,15] DNA, in particular, has been explored extensively as a tunable chemical linker between nanoparticles, where Watson−Crick base pairing organizes nanoparticles in solution into discrete structures or large-area lattices.[16−19] The length and arrangement of unit cells can be initially controlled through design of specific base pair sequences. These lengths and arrangements can then be actively tuned through the addition of restriction enzymes or transcription factors that target specific recognition sequences, by external fuel strands that interact with particular DNA structures such as stem loops or rotaxanes, by light when photoswitches are directly synthesized into the DNA strands, or by nonspecific external stimuli such as temperature, pH, and ionic strength.[20−24] Examples of switchable plasmonic chiral assemblies to date include assemblies anchored to a substrate, heterodimers, and tetrahedra.[25−27] Lithographic photoswitchable chiral metamaterials have also been demonstrated.[28]

Tetrahedral DNA structures with nanoparticles attached at the vertices form one of the most-studied chiral plasmonic nanoparticle assemblies. As discussed in previous literature, asymmetry can be designed into this structure through the use of particles of different shapes, sizes, or compositions (substitutional chirality), or through the use of unequal interparticle distances (configurational chirality).[4,6,7,29] Specific implementations in the tetrahedral geometry include substitutional tetrahedra with four different size Au nanoparticles at the vertices and symmetric edge lengths, and configurational tetrahedra with four similarly sized nanoparticles and different edge lengths.[4,6,9] It has recently been shown both theoretically and experimentally in plasmonic tetrahedra that chirality induced by configurational asymmetry produces a more significant CD response than that induced by substitutional asymmetry.[6,29]

In this paper, we use simulation methods to explore the influence of symmetry breaking on CD spectra using a variant on the tetrahedron structure consisting of two pairs of nanoparticles with one unequal edge length. In this structure, chirality is determined by motion along one arm. We explore

Received: July 21, 2014
Published: October 22, 2014

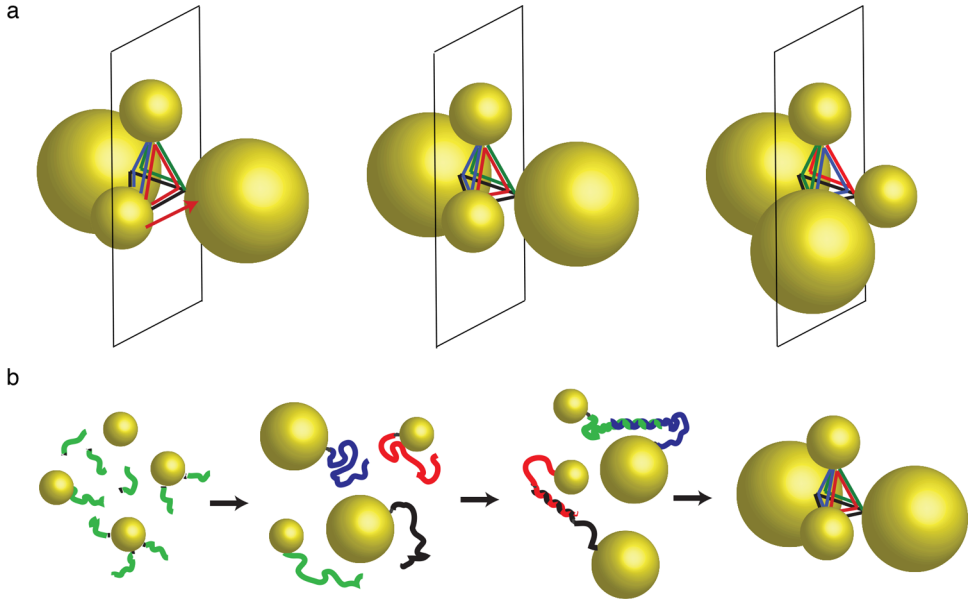

Figure 1. Schematic of DNA-assembled chiral pyramids. (a) Achiral pyramid with two different sizes of nanoparticles and equal edge lengths (left). Shortening the red-black edge breaks the mirror plane and induces chirality (middle). Shortening the blue-black edge produces the opposite enantiomer (right). (b) Schematic overview showing how monoconjugated DNA-Au nanoparticles combine to form a pyramid, with each DNA strand forming one face of the final structure.

the connection between CD spectra and structure of the tetrahedron using realistic synthetic constraints and compare this structure to substitutional and configurational designs. The structure is spectrally sensitive to small changes in distance through wavelength, intensity, and changes in sign. We then discuss the design constraints on the system, showing that the pairs of nanoparticles may consist of different materials and that it is not necessary for their resonances to match. We find that systems consisting of different plasmonic metals are more sensitive to structural changes but also exhibit reduced CD intensity compared to systems with nanoparticles of the same material. This tetrahedral geometry holds synthetic advantages over substitutional and configurational geometries and may find application as a switchable metamaterial or nanoscale ruler.

RESULTS

The design we present utilizes the principle of symmetry breaking to induce tunable chirality in a tetrahedral assembly of nanoparticles. We first consider the structure shown schematically in Figure 1, with straight lines depicting the DNA frame for clarity. On the left is an achiral tetrahedron where the tetrahedron frame is designed with equal edge lengths and two different sizes of Au nanoparticles are attached to the vertices. This structure is not optically active as it contains mirror planes and therefore improper rotation axes. Chirality is induced by shortening one edge of the DNA frame to break the mirror planes, as depicted with the red arrow forming the middle schematic. Shortening the opposite arm (blue-black side in Figure 1) creates the enantiomer, as shown in the third schematic of Figure 1a. The magnitude of the CD signal is correlated to the difference between the edge lengths: the greater the difference between the targeted edge length and the nontargeted edge lengths, the stronger the chiroptical effect.

To understand some of the advantages of this design, it is useful to consider the synthetic process that has previously been employed to assemble tetrahedra of nanoparticles, shown schematically in Figure 1b.[4] Previous work has demonstrated the synthesis of tetrahedral assemblies with four different Au nanoparticle sizes attached to the vertices, and with asymmetry built directly into the frame, but it is straightforward to describe the extension to the system considered here.[4−6] First Au nanoparticles of a given diameter are combined with thiol-modified DNA. This forms a statistical mixture of products, including unmodified Au nanoparticles, monoconjugated DNA-Au nanoparticles, and higher order oligonucleotide conjugates. The monoconjugated DNA-Au product is isolated from the solution using a purification step such as high performance liquid chromatography (HPLC), gel electrophoresis, or density gradient centrifugation.[4,5] This procedure is repeated to create four distinct solutions of monoconjugated DNA-Au particles: in this case, two with 10 nm particles and two with 20 nm particles, each with a different DNA sequence. The solutions are combined in pairs and then into one mixture to form the final tetrahedral structure. As depicted in Figure 1b, each face of the tetrahedron is formed by one of the original DNA strands, which is complementary to a portion of the other three. The nanoparticles are located at the vertices of the tetrahedron, attached by a flexible thiolated linker.

Previous work on DNA tetrahedra has demonstrated that, due to the design of DNA with helical turns at the corners of the frame, enantiomers form in >95% enantiomeric excess.[30,31] The enantiomer formed in a static structure is therefore determined through the initial synthetic design, either through the choice of different nanoparticle sizes or through the original length of the DNA strands used during assembly. The number of base pairs is chosen to have an integral number of half helical turns per side for stability. This makes the formation of tetrahedra with six unequal edge lengths challenging, as the structures must both be thermodynamically favorable and contain sufficiently small interparticle distances for effective plasmonic coupling. In the design presented here, only one edge of the tetrahedron frame needs to be of a different length from the other five, permitting the formation of more stable structures while preserving strong optical activity. This hybrid

dx.doi.org/10.1021/ph5002632 | ACS Photonics 2014, 1, 1189−1196

design thus potentially affords both synthetic ease and functional optical response.

To study the effect of symmetry breaking on this initial tetrahedron design, we utilized a coupled dipole approximation simulation method with realistic parameters dictated by experiment, similar to the methods reported elsewhere.[7,32] The model fixes the dimensions of the DNA frame (10 nm on all edges except for the symmetry-breaking edge) and positions the nanoparticles off of the vertices of the tetrahedron as though they were attached by a linker molecule. The DNA is not modeled explicitly, except to determine the positions of the nanoparticles spatially in relationship to the frame and linker. As the distance is changed along the targeted edge, it is kept fixed on the nontargeted edges, and the positions of the nanoparticles in space are recalculated for each new configuration. The nanoparticles are 10 and 20 nm in diameter, and the polarizability of each Au nanoparticle is modeled as a perfect sphere using Johnson and Christy data for the wavelength-dependent complex permittivity.[33] The assemblies are assumed to be in water, as the refractive index of a low concentration tris buffer is not significantly different. We calculate the circular dichroism of the system as the difference in molar extinction under left and right handed circularly polarized light, integrated over all angles of incidence.

$$\mathrm{CD} = \langle \sigma_{\mathrm{LH}} - \sigma_{\mathrm{RH}} \rangle_{\Omega}$$

The calculations account for the freely rotating tetrahedron in solution by rotating the direction of illumination over all of the possible angles, since this is mathematically equivalent to rotating the structure. Further details of the calculation method are provided in the Supporting Information (SI).

There are a few significant differences between considerations of this system and lithographically designed chiral structures. First, in the latter case, handedness is typically dependent on the direction of illumination.[6,7] In the system under consideration here, we integrate over all angles of incidence similar to a structure rotating in solution. Second, we deliberately focus on small nanoparticles here, similar to those that are synthetically accessible, placing these assemblies in a different coupling regime than assemblies of larger nanoparticles and small interparticle spacings which have been explored lithographically.[9]

Figure 2 shows the result of calculations of the extinction and circular dichroism of this tetrahedron design as the distance on the symmetry-breaking arm is changed. This is analogous to the experiments described earlier where an external stimulus targets one edge of the tetrahedron. Figure 2a plots the calculated extinction of this assembly for linearly polarized excitation, showing there is no significant change in the peak wavelength or intensity as the configuration of this assembly changes. In contrast, Figure 2b shows the CD spectrum as the distance along the symmetry-breaking arm lengthens, exhibiting significant spectral tunability. Plasmon coupling as visible in extinction is therefore not a necessary prerequisite for plasmonic CD response: by detecting the difference between polarizations, CD is a more sensitive technique over this length scale than extinction. The CD spectrum exhibits a characteristic bisignate shape. The intensity of the CD spectrum increases as the distance of the symmetry-breaking arm is modified from the symmetric length of 10 nm, with the most intensity at the shortest distance considered here (6 nm). As plasmonic coupling scales with the distance between elements, it is expected that bringing the plasmonic nanoparticles closer together will produce a stronger response. Notably, the CD spectrum of the assembly switches sign when the targeted arm is shorter/longer than the symmetric length of 10 nm. Control

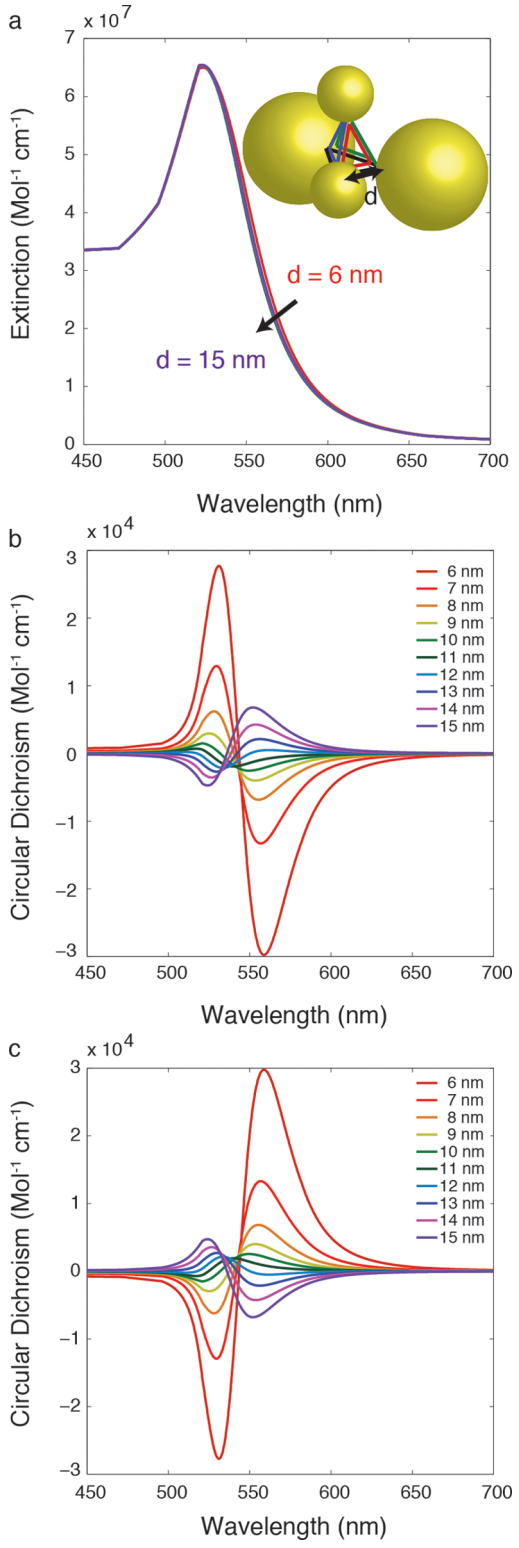

Figure 2. Calculated extinction and CD spectra for pyramids as distance changes along one edge. (a) Extinction of pyramid calculated with linearly polarized light. (b) Circular dichroism spectra for enantiomer pictured in the inset of (a). (c) Circular dichroism for the opposite enantiomer. The particle diameters are 10 and 20 nm and the nontargeted edge lengths are fixed at 10 nm.

dx.doi.org/10.1021/ph5002632 | ACS Photonics 2014, 1, 1189−1196

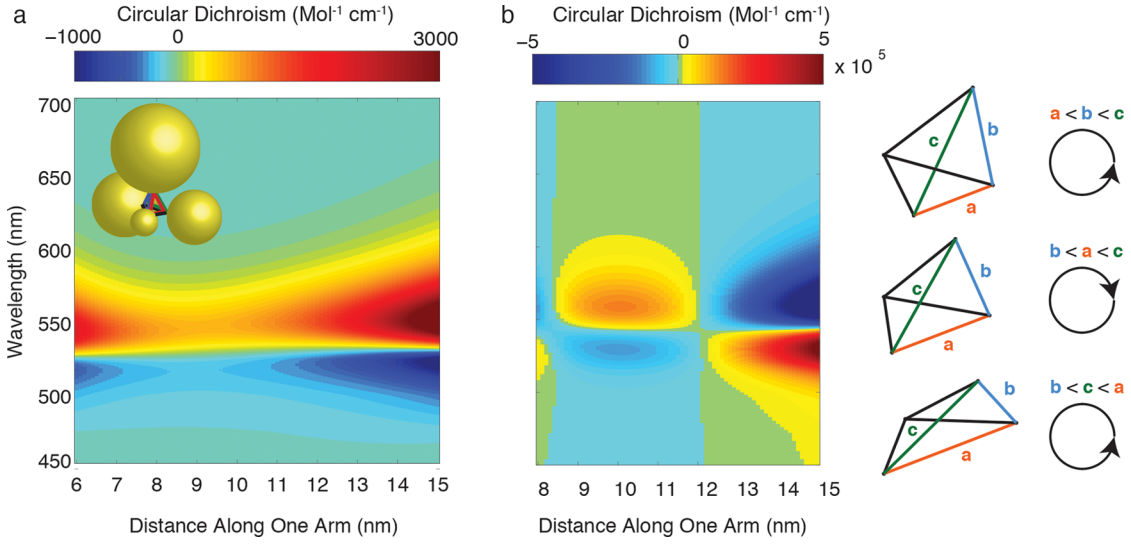

Figure 3. CD spectra from substitutional and configurational chiral pyramids. (a) CD from substitutional pyramid with nanoparticle diameters of 5, 10, 15, and 20 nm, where the distance along one arm changes. The other edges are kept fixed at 10 nm. (b) CD from a pyramid where asymmetry is designed into one face. All of the nanoparticles are 20 nm in diameter. The corresponding frame is shown schematically without the nanoparticles for clarity. Length *a* is the targeted edge and varies in length. Lengths *b* and *c* are 8 and 12 nm, respectively, and the other three edges are fixed at 10 nm.

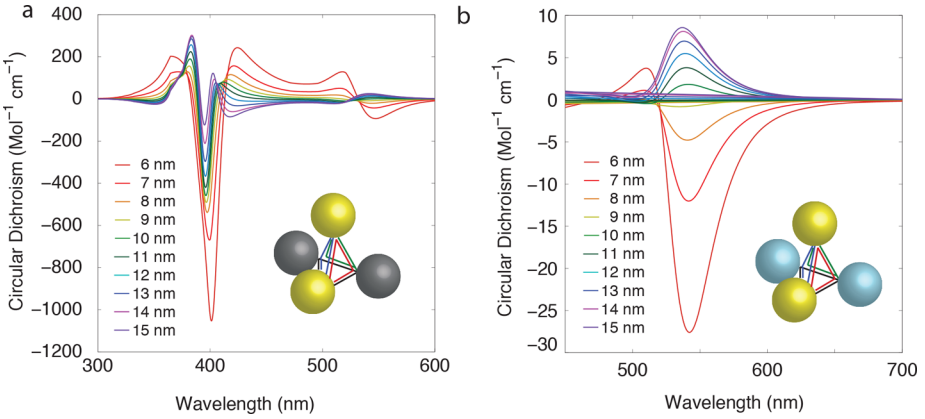

Figure 4. Calculations of pyramids with other materials. (a) Symmetry breaking pyramid design with Au and Ag nanoparticles. The distance between one Au particle and one Ag particle is varied (red-black edge) while the others are fixed at 10 nm. All nanoparticles are 20 nm in diameter. (b) Symmetry breaking pyramid design with two Au nanoparticles and two TiO_2 nanoparticles. The distance between one Au nanoparticle and one TiO_2 is varied while the others are fixed at 10 nm. All nanoparticles are 20 nm in diameter.

calculations where the edge between nanoparticles of the same size is shortened, which does not break the mirror planes of the assembly, do not exhibit CD and are shown in Figure S2 of the SI.

The sign of the CD spectrum also switches depending on which symmetry-breaking arm is targeted. Figure 2c shows the effect of shortening the other symmetry-breaking edge of the tetrahedron to form the enantiomer of Figure 2b (blue-black lines in Figure 1). Changing the distance of this arm from 6 to 15 nm similarly switches the handedness, but in the opposite direction from the structure in Figure 2b. As will be discussed in more detail later, the intensity, sign, and spectral characteristics of the CD spectrum of this assembly encodes nanoscale structural information about the assembly under distortion.

The ability of this structure to switch handedness is directly related to the breaking of the mirror plane illustrated in Figure 1a. Figure 3a shows the results of a similar calculation on a substitutionally asymmetric tetrahedron, using nanoparticles of 5, 10, 15, and 20 nm diameter. The data is represented as a color map here, showing the CD spectrum (*y*-axis) as the distance along one arm is changed (*x*-axis). Overall, the magnitude of the calculated CD spectrum is significantly smaller than in the configurational case. The direction of the CD does not switch as the handedness is determined by the spatial arrangement of the four nanoparticles rather than asymmetry in the frame. However, the CD response is most intense at the two extremes in distance, indicating that the CD is strengthened by the additional asymmetry.

The principle of symmetry breaking to switch handedness can be used to design more complex structures, such as the configurational asymmetry design studied in Figure 3b. In this case, the four nanoparticles are the same size (20 nm) and asymmetry is built into one face of the tetrahedron. The length of side *a* changes, side *b* is fixed at 8 nm, and side *c* is fixed at 12 nm. The remaining three sides are 10 nm in length. For clarity, a schematic of the frame without the nanoparticles is shown. The length of side *a* is changed from 8 to 15 nm, as shorter distances result in touching nanoparticles. As the ratio of side lengths changes from $a < b < c$ to $b < a < c$, the handedness of

dx.doi.org/10.1021/ph5002632 | ACS Photonics 2014, 1, 1189−1196

the tetrahedron switches. As it transitions into $b < c < a$, the handedness reverses a second time.

Notably, this design does not require that the nanoparticles have matching resonances. As CD arises from the spatial configuration combined with the different extinction properties of the nanoparticles, it is not necessary to use identical nanoparticles, or even all plasmonic nanoparticles. Figure 4 explores two cases where the symmetry is broken by using two different materials rather than different diameters of Au nanoparticles. The setup is identical: we start with an achiral assembly of two Au and two other (Ag or TiO_2) nanoparticles (all 10 nm in diameter) and induce chirality by breaking the mirror plane by shortening or lengthening one edge. Figure 4a shows the predicted response for the Au/Ag pair.[34] CD is predicted to occur at the Au resonance at 520 nm as in the structures in Figure 2, and also near the Ag resonance near 400 nm. The CD features around the Ag resonance are more intense, as has been observed in plated Ag assembled structures.[3] Significant tunability of the wavelength is observed with distance as well, as will be discussed in more detail later. Figure 4b illustrates the case where the opposite nanoparticles are not plasmonic, using TiO_2 as the opposite pair. In this case the CD spectrum around the Au resonance at 520 nm is considerably weaker, but still present, and still switches handedness with changing distance along the targeted arm. This points to the possibility that a dimer of Au nanoparticles embedded in a chiral dielectric medium may still exhibit CD. We note that this is consistent with experimental measurements on structures with substitutional asymmetry using combinations of Ag, Au, and quantum dots.[5,26]

A natural application of this structure is as a nanoscale optical ruler to retrieve structural information about the assembly under dynamic conditions. Tunable DNA tetrahedra have been demonstrated using DNA hairpins that are sensitive to stimuli such as protons, ATP, or Hg ions, as well as photosensitive oligonucleotides modified with azobenzene moieties.[35−37] In this case, information about the nanoscale structure can be retrieved by monitoring the sign and spectral positions of the peaks in the CD spectrum in Figure 2 that are strongly dependent on distance along the targeted arm. We have already identified from Figure 2 that the interactions on different sides of the tetrahedron can be distinguished by the sign of the resulting CD spectrum, as seen by comparing Figure 2b and 2c. Figure 5 shows the calculated peak positions from the spectra in Figure 2, comparing the tetrahedron to a dimer of 20 nm particles separated by the same distance. The CD spectra maxima and minima are shown as the red and blue lines, respectively, as both the peak and the valley could be reliably determined from each spectrum. The greatest shift in the spectral position of the CD maxima and minima occurs at distances close to the symmetric length of 10 nm. This is in contrast to a standard plasmon ruler based on extinction in dimers, where the greatest shift in spectral position occurs at the shortest distances. For example, as the distance along the targeted arm changes from 10 to 11 nm, the valley of the CD spectrum changes by 10 nm, from 550 to 540 nm. As the edge becomes significantly shorter (or longer) than 10 nm, the spectral position dependence is weaker in wavelength; changing the distance from 7 to 8 nm changes the CD spectral peak and valley by only 1 nm. The peak position in linear extinction from both the tetrahedron and the 20 nm Au dimer exhibits little change in spectral position with respect to wavelength. The structure therefore functions as a chiral plasmon ruler where

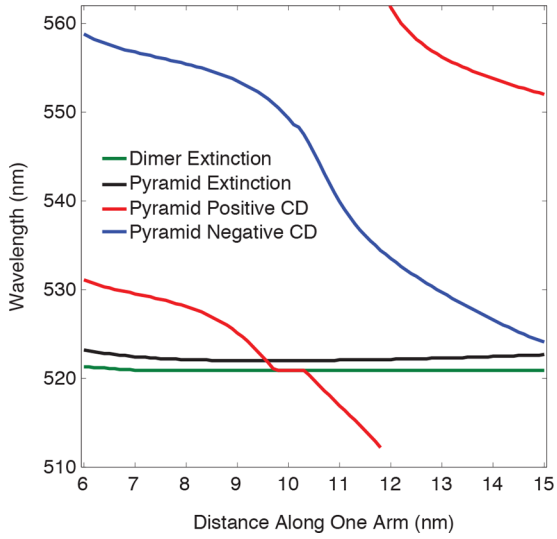

Figure 5. Calculated peak positions comparing pyramids to dimers. The peak positions of both the positive and negative spectral CD feature are calculated as the distance along one arm changes. The particle diameters are 10 and 20 nm and the nontargeted edge lengths are fixed at 10 nm. The peak positions of the linear extinction spectrum in this pyramid are shown for reference. A similar calculation was performed for the extinction of a dimer of 20 nm Au particles where the interparticle distance is tuned over the same range.

the wavelength dependence and sign of the spectroscopic CD signal provide information about the nanoscale distances in the assembly.

Additional three-dimensional information can now be understood from the assembly in Figure 4a of the Au−Ag pairs. Figure 6 shows the evolution and sign of these peak positions as the length of the targeted arm is changed. Figure 6a represents the data as a color map over a broad spectral range, with the overlaid lines representing the peak position of the CD local maxima (black) or minima (white). Figure 6b,c shows the spectral dependence of each of these peak positions in more detail. In this case, monitoring different spectral regions allows for the retrieval of distance information across a broader range of distances. To monitor a change from 7 to 8 nm in distance, monitoring the spectral peak near 515 nm now shifts by 5 nm. Other CD peaks in this range have spectral shifts from 2 to 3 nm. For a targeted arm distance change from 9 to 10 nm, one of the valleys shifts from 537.6 to 520.9 nm (where the CD switches handedness). Therefore, different CD bands could be monitored to span a larger range of distances along the targeted arm, while preserving the same high-resolution as the structure in Figure 5. Figure S3 in the SI shows the change in maximum and minimum in the substitutional and configurational chiral tetrahedra discussed in Figure 3, illustrating the importance of the change in handedness in retrieving nanoscale information.

The ideal self-assembled, tunable structure is one that shows dramatic changes in response to the desirable external stimulus, but is stable against small fluctuations in solution or fabrication imperfections.[38,39] Stability against both of these parameters will be critical for application either as a three-dimensional sensor or as a switchable chiral metamaterial. Figure 7a shows the CD spectrum of the perfect tetrahedron explored in Figures 2 and 5, represented as a color map with length of the symmetry-breaking arm along the x-axis and wavelength along the y-axis. The bisignate nature of the spectrum is visible in the

dx.doi.org/10.1021/ph5002632 | ACS Photonics 2014, 1, 1189−1196

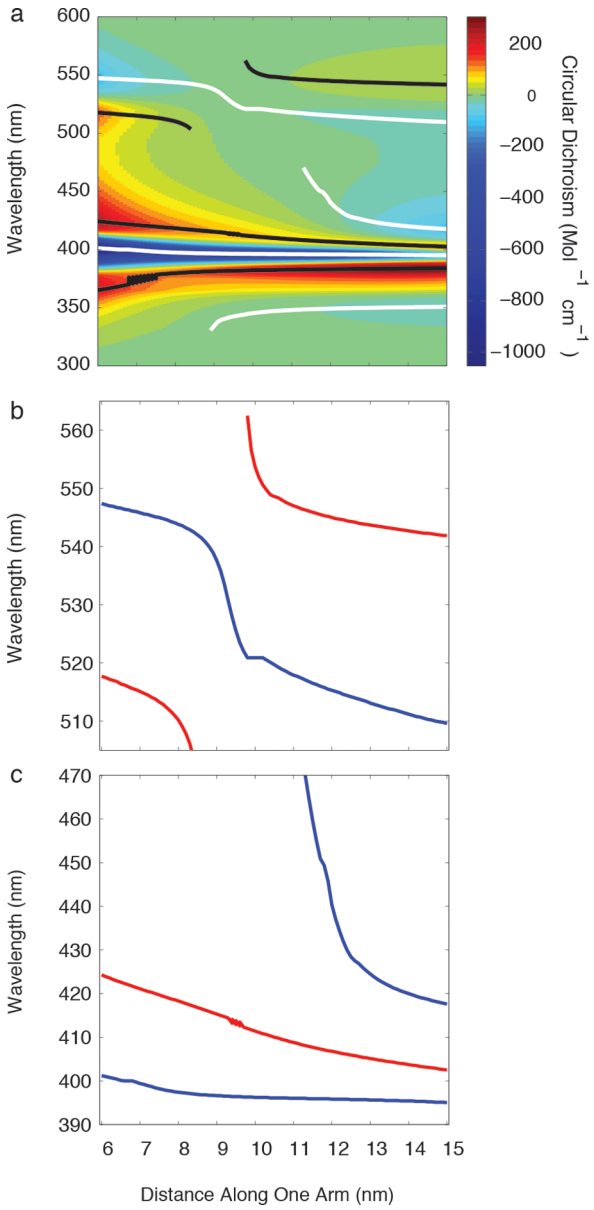

Figure 6. Calculated peak positions from Au/Ag pyramid. (a) Colormap showing the CD spectrum from the structure shown in Figure 4a. The black and white lines denote the local maxima and minima, respectively. (b, c) Blown up figures showing the change in the maxima and minima near the resonance of the Au nanoparticles (b) and the Ag nanoparticles (c).

different colors, and the sign of the CD spectrum switches as the length of the targeted arm increases.

Under realistic synthetic conditions, nanoparticles will exhibit variation in diameter. Figure 7b shows the same calculation as Figure 7a considering polydispersity of the nanoparticle diameters. For each simulation, nanoparticle diameters were chosen from a normal distribution assuming 10% standard deviation and a mean size of either 10 or 20 nm. This distribution is comparable or larger than typically observed experimentally in nanoparticles. In the experimental system, the spatial arrangement of each nanoparticle relative to each other within the assembly is determined by the initial DNA conjugation step (as each DNA strand contains a specific base pair sequence that can only bind one way). The two smaller nanoparticles, regardless of polydispersity, will attach to the same two points of the tetrahedron, and similarly for the two larger nanoparticles. Therefore, the calculation was performed by first constructing a tetrahedron with nanoparticle diameters drawn from the distribution, and then changing the distance along a targeted edge for a given assembly while integrating over all angles of incident light. As CD is typically an ensemble measurement, the spectra from 50 sets of nanoparticle diameters were averaged to produce Figure 7b.

As can be seen by comparing Figure 7a and b, polydispersity of nanoparticle diameters does not have a significant effect on the CD tunability with symmetry breaking. The intensity of the CD spectrum depends strongly on the diameter of the nanoparticles at these distances, increasing substantially with larger particles. Even if the nanoparticle diameters are chosen to be closer together with some overlap in their distributions, such as 10 and 15 nm, a sufficient number of tetrahedra in the set have the correct handedness and the CD spectra are not significantly noisier, as shown in the SI. Polydispersity of nanoparticle diameter is, thus, not expected to significantly impact the optical design.

The distance along the nontargeted arms, and particularly the flexible linker between the DNA and the Au nanoparticle, will also vary, and Figure 7c shows the result of calculations considering these fluctuations. The distances on the nontargeted sides are chosen from a normal distribution with a mean length of 10 nm and a standard deviation of 1 nm. In this calculation, a single tetrahedron is assumed to be constantly fluctuating while the distance on the targeted arm is modified in response to the stimulus. The calculation is performed where at each specified distance of the targeted arm (6−15 nm) different edge lengths for each of the nontargeted arms are chosen randomly from the distribution. This procedure is repeated 50 times, and the average spectrum is shown in Figure 7c. The main features of the symmetry breaking tetrahedron design are preserved when considering distance fluctuations, although there is more variation than in the polydispersity calculations. The spectrum is noisier, since for a single tetrahedron the length of the nontargeted arms when the targeted arm is 6 nm is not the same as the length of the nontargeted arms at a targeted distance of 6.1 nm. Nevertheless, the sign of the handedness inverts as the targeted arm's length is changed, the peak spectral positions of the CD spectrum shift similarly to those in Figure 7a, and the intensity of the CD spectrum is highest for the shortest edge length. Since in a realistic experiment these fluctuations will occur rapidly and will include many more than 50 variations, we conclude that this design is relatively stable against nonspecific modifications.

■ CONCLUSIONS

The chiral plasmonic assemblies described here are designed using symmetry breaking principles to tune and invert the CD signal. This geometry with two pairs of nanoparticles and one asymmetric edge length is a viable option for experimental systems, requiring only a single stimuli-responsive portion of the structure to tune and switch the spectral position, intensity, and sign of the CD signal. This makes the chiral tetrahedron an effective plasmon ruler, capable of detecting small changes in nanoscale structure at longer distances than are observable in extinction. The pairs of nanoparticles may be the same material with different sizes, or different materials that are not all plasmonic. We find that using two different materials increases the sensitivity over a longer range of distances but also decreases the overall magnitude of the CD signal. Finally, we

dx.doi.org/10.1021/ph5002632 | ACS Photonics 2014, 1, 1189−1196

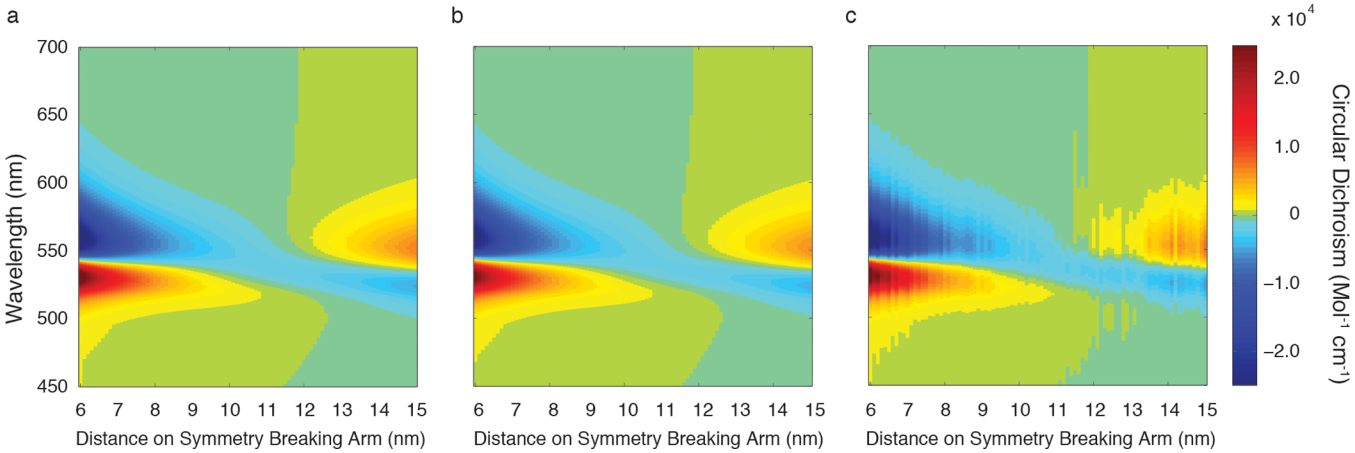

Figure 7. Calculations of CD spectra with imperfect fabrication. (a) Calculated CD from a pyramid with 10 and 20 nm particle sizes and all nontargeted arms fixed at 10 nm. (b) Calculated CD from a pyramid including polydispersity in nanoparticle diameters. (c) Calculated CD from a pyramid including fluctuating distances on nontargeted arms. The calculations in b and c are averaged over 50 iterations.

find that if two different sizes of nanoparticles are used as the two pairs, the sizes must be sufficiently different from each other that polydispersity within the sample does not change the symmetry of the structure. In addition to sensing nanoscale structural changes, this design may find use as a switchable fluid metamaterial.

METHODS

All calculations are performed using home-written coupled dipole simulations, similar to those described elsewhere in the literature.[29,32] More details are provided in the SI.

ASSOCIATED CONTENT

Supporting Information

The simulation method is described in detail, and calculated spectra for control designs is presented. This material is available free of charge via the Internet at http://pubs.acs.org.

AUTHOR INFORMATION

Notes

The authors declare no competing financial interest.

ACKNOWLEDGMENTS

We are grateful to Mario Hentschel for useful discussions. This material is based upon work supported by the National Science Foundation under Grant DMR-1344290.

REFERENCES

(1) Wang, Y.; Xu, J.; Wang, Y.; Chen, H. Emerging chirality in nanoscience. *Chem. Soc. Rev.* **2013**, *42*, 2930−2962.
(2) Valev, V. K.; Baumberg, J. J.; Sibilia, C.; Verbiest, T. Chirality and chiroptical effects in plasmonic nanostructures: Fundamentals, recent progress, and outlook. *Adv. Mater.* **2013**, *25*, 2517−2534.
(3) Kuzuk, A.; Schreiber, R.; Fan, Z.; Pardatscher, G.; Roller, E.-M.; Högele, A.; Simmel, F. C.; Govorov, A. O.; Liedl, T. DNA-based self-assembly of chiral plasmonic nanostructures with tailored optical response. *Nature* **2012**, *483*, 311−314.
(4) Mastroianni, A. J.; Claridge, S. A.; Alivisatos, A. P. Pyramidal and chiral groupings of gold nanocrystals assembled using DNA scaffolds. *J. Am. Chem. Soc.* **2009**, *131*, 8455−8459.
(5) Yan, W.; Xu, L.; Xu, C.; Ma, W.; Kuang, H.; Wang, L.; Kotov, N. A. Self-assembly of chiral nanoparticles with strong R/S optical activity. *J. Am. Chem. Soc.* **2012**, *134*, 15114−15121.
(6) Shen, X.; Asenjo-Garcia, A.; Liu, Q.; Jiang, Q.; Garcia de Abajo, F. J.; Liu, N.; Ding, B. Three-dimensional plasmonic chiral tetramers assembled by DNA origami. *Nano Lett.* **2013**, *13*, 2128−2133.
(7) Fan, Z.; Zhang, H.; Govorov, A. O. Optical properties of chiral plasmonic tetramers: Circular dichroism and multipole effects. *J. Phys. Chem. C* **2013**, *117*, 14770−14777.
(8) Ma, W.; Kuang, H.; Wang, L.; Xu, L.; Chang, W.-S.; Zhang, H.; Sun, M.; Zhu, Y.; Zhao, Y.; Liu, L.; Xu, C.; Link, S.; Kotov, N. A. Chiral plasmonics of self-assembled nanorod dimers. *Sci. Rep.* **2013**, *3*, 1934.
(9) Hentschel, M.; Schäferling, M.; Weiss, T.; Liu, N.; Giessen, H. Three-dimensional chiral plasmonic oligomers. *Nano Lett.* **2012**, *12*, 2542−2547.
(10) Yan, W.; Ma, W.; Kuang, H.; Liu, L.; Wang, L.; Xu, L.; Xu, C. Plasmonic chirogenesis from gold nanoparticles superstructures. *J. Phys. Chem. C* **2013**, *117*, 17757−17765.
(11) Pendry, J. B. A chiral route to negative refraction. *Science* **2004**, *306*, 1353−1355.
(12) Gansel, J. K.; Thiel, M.; Rill, M. S.; Decker, M.; Bade, K.; Saile, V.; von Freymann, G.; Linden, S.; Wegener, M. Gold helix photonic metamaterial as broadband circular polarizer. *Science* **2009**, *325*, 1513−1515.
(13) Tang, Y.; Cohen, A. E. Enhanced enantioselectivity in excitation of chiral molecules by superchiral light. *Science* **2011**, *332*, 333−336.
(14) Mühlig, S.; Cunningham, A.; Dintinger, J.; Scharf, T.; Bürgi, T.; Lederer, F.; Rockstuhl, C. Self-assembled plasmonic metamaterials. *Nanophotonics* **2013**, *2*, 211−240.
(15) Kuzyk, A.; Schreiber, R.; Zhang, H.; Govorov, A. O.; Liedl, T.; Liu, N. Reconfigurable 3D plasmonic metamolecules. *Nat. Mater.* **2014**, *13*, 862−866.
(16) Wu, X.; Xu, L.; Liu, L.; Ma, W.; Yin, H.; Kuang, H.; Wang, L.; Xu, C.; Kotov, N. A. Unexpected chirality of nanoparticle dimers and ultrasensitive chiroplasmonic bioanalysis. *J. Am. Chem. Soc.* **2013**, *135*, 18629−18636.
(17) Tan, S. J.; Campolongo, M. J.; Luo, D.; Cheng, W. Building plasmonic nanostructures with DNA. *Nat. Nanotechnol.* **2011**, *6*, 268−276.
(18) Young, K. L.; Ross, M. B.; Blaber, M. G.; Rycenga, M.; Jones, M. R.; Zhang, C.; Senesi, A. J.; Lee, B.; Schatz, G. C.; Mirkin, C. A. Using DNA to design plasmonic metamaterials with tunable optical properties. *Adv. Mater.* **2014**, *26*, 653−659.
(19) Macfarlane, R. J.; Lee, B.; Jones, M. R.; Harris, N.; Schatz, G. C. Nanoparticle superlattice engineering with DNA. *Science* **2011**, *334*, 204−208.
(20) Sonnichsen, C.; Reinhard, B. M.; Liphardt, J.; Alivisatos, A. P. A molecular ruler based on plasmon coupling of single gold and silver nanoparticles. *Nat. Biotechnol.* **2005**, *23*, 741−745.

(21) Morimura, H.; Tanaka, S.-I.; Ishitobi, H.; Mikami, T.; Kamachi, Y.; Kondoh, H.; Inouye, Y. Nano-analysis of DNA conformation changes induced by transcription factor complex binding using plasmonic nanodimers. *ACS Nano* **2013**, *7*, 10733−10740.
(22) Maye, M. M.; Kumara, M. T.; Nykypanchuk, D.; Sherman, W. B.; Gang, O. Switching binary states of nanoparticle superlattices and dimer clusters by DNA strands. *Nat. Nanotechnol.* **2010**, *5*, 116−120.
(23) Lermusiaux, L.; Sereda, A.; Portier, B.; Larquet, E.; Bidault, S. Reversible switching of the interparticle distance in DNA-templated gold nanoparticle dimers. *ACS Nano* **2012**, *6*, 10992−10998.
(24) Cecconello, A.; Lu, C.-H.; Elbaz, J.; Willner, I. Au nanoparticle/DNA rotaxane hybrid nanostructures exhibiting switchable fluorescence properties. *Nano Lett.* **2013**, *13*, 6275−6280.
(25) Schreiber, R.; Luong, N.; Fan, Z.; Kuzyk, A.; Nickels, P. C.; Zhang, T.; Smith, D. M.; Yurke, B.; Kuang, W.; Govorov, A. O.; Liedl, T. Chiral plasmonic DNA nanostructures with switchable circular dichroism. *Nat. Commun.* **2013**, *4*, 2948.
(26) Yan, W.; Xu, L.; Ma, W.; Liu, L.; Wang, L.; Kuang, H.; Xu, C. Pyramidal sensor platform with reversible chiroptical signals for DNA detection. *Small* **2014**, DOI: 10.1002/smll.201401641.
(27) Yan, Y.; Chen, J. I. L.; Ginger, D. S. Photoswitchable oligonucleotide-modified gold nanoparticles: Controlling hybridization stringency with photon dose. *Nano Lett.* **2012**, *12*, 2530−2536.
(28) Zhang, S.; Zhou, J.; Park, Y.-S.; Rho, J.; Singh, R.; Nam, S.; Azad, A. K.; Chen, H.-T.; Yin, X.; Taylor, A. J.; Zhang, X. Photoinduced handedness switching in terahertz chiral metamolecules. *Nat. Commun.* **2012**, *3*, 942.
(29) Fan, Z.; Govorov, A. O. Plasmonic circular dichroism of chiral metal nanoparticle assemblies. *Nano Lett.* **2010**, *10*, 2580−2587.
(30) Goodman, R. P.; Heilemann, M.; Doose, S.; Erben, C. M.; Kapanidis, A. N.; Turberfield, A. J. Reconfigurable, braced, three-dimensional DNA nanostructures. *Nat. Nanotechnol.* **2008**, *3*, 93−96.
(31) Goodman, R. P.; Schaap, I. A. T.; Tardin, C. F.; Erben, C. M.; Berry, R. M.; Schmidt, C. F.; Turberfield, A. J. Rapid chiral assembly of rigid DNA building blocks for molecular nanofabrication. *Science* **2005**, *310*, 1661−1665.
(32) Auguié, B.; Alonso-Gómez, J. L.; Guerrero-Martínez, A.; Liz-Maran, L. M. Fingers crossed: Optical activity of a chiral dimer of plasmonic nanorods. *J. Phys. Chem. Lett.* **2011**, *2*, 846−851.
(33) Johnson, P. B.; Christy, R. W. Optical constants of the noble metals. *Phys. Rev. B* **1972**, *6*, 4370−4379.
(34) Sheikholeslami, S.; Jun, Y.; Jain, P. K.; Alivisatos, A. P. Coupling of optical resonances in a compositionally asymmetric plasmonic nanoparticle dimer. *Nano Lett.* **2010**, *10*, 2655−2660.
(35) Pei, H.; Liang, L.; Yao, G.; Li, J.; Huang, Q.; Fan, C. Reconfigurable three-dimensional DNA nanostructures for the construction of intracellular logic sensors. *Angew. Chem.* **2012**, *124*, 9154−9158.
(36) Han, D.; Huang, J.; Zhu, Z.; Yuan, Q.; You, M.; Chen, Y.; Tan, W. Molecular engineering of photoresponsive three-dimensional DNA nanostructures. *Chem. Commun.* **2011**, *47*, 4670−4672.
(37) Sadowski, J. P.; Calvert, C. R.; Zhang, D. Y.; Pierce, N. A.; Yin, P. Developmental self-assembly of a DNA tetrahedron. *ACS Nano* **2014**, *8*, 3521−3529.
(38) Fan, Z.; Govorov, A. O. Helical metal nanoparticle assemblies with defects: Plasmonic chirality and circular dichroism. *J. Phys. Chem. C* **2011**, *117*, 13254−13261.
(39) Mastroianni, A. J.; Sivak, D. A.; Geissler, P. L.; Alivisatos, A. P. Probing the conformational distributions of subpersistence length DNA. *Biophys. J.* **2009**, *97*, 1408−1417.